PHYSICAL REVIEW B **85**, 125426 (2012)

Theory of orthogonal interactions of CO molecules on a one-dimensional substrate

Chungwei Lin,[1] Min Feng,[1] Jin Zhao,[1,2] Pepa Cabrera-Sanfelix,[3,4,5]
Andres Arnau,[3,4,5] Daniel Sánchez-Portal,[3,4,5] and Hrvoje Petek[1]
[1]*Department of Physics and Astronomy and Petersen Institute of NanoScience and Engineering, University of Pittsburgh, Pittsburgh, Pennsylvania 15260, USA*
[2]*Physics Department, Hefei National Laboratory for Physical Sciences at Microscale, University of Science and Technology of China, Hefei, Anhui, China*
[3]*Donostia International Physics Center (DIPC), San Sebastin/Donostia 20018, Spain*
[4]*Centro de Física de Materiales (CFM-MPC), CSIC-UPV/EHU, San Sebastin 20018, Spain*
[5]*Departamento de Física de Materiales UPV/EHU, Facultad de Quimica, San Sebastián 20080, Spain*
(Received 28 July 2011; revised manuscript received 8 March 2012; published 20 March 2012)

A minimal model based on density-functional theory is proposed and solved to explain the unusual chemisorption properties of carbon-monooxide (CO) molecules on Cu(110)-(2 × 1)-O quasi-one-dimensional (1D) surface reported in Feng *et al*. [ACS Nano **5**, 8877 (2011)]. The striking features of CO adsorption include (1) the strong lifting of the host Cu atom by 1 Å, and (2) the highly anisotropic CO-CO interaction leading to self-assembly into a nanograting structure. Our model implies that the 1D nature of the surface band is the key to these two features. We illustrate how formation of a chemical bond through specific orbital interactions between an adsorbate and 1D dispersive states of the substrate can impact the surface geometrical and electronic structure.

DOI: 10.1103/PhysRevB.85.125426 PACS number(s): 68.43.−h, 64.75.Yz

I. INTRODUCTION

One of the most important topics in surface science is the relationship between molecule adsorption and the mode of intermolecular interaction. When molecules or adatoms are adsorbed on an isotropic two-dimensional (2D) metal surface, the standard picture can be summarized as follows.[1] The adsorption occurs when the process gains sufficient energy from the hybridization and charge transfer between orbitals of substrate and adsorbate.[2,3] Because the adsorption energy is of the order electron volt (eV) and is usually the largest energy scale, the host atom-adsorbate complex can be treated as the basic unit, a quasimolecule, of the system with an associated dipole moment in the range from a tenth to a few $e\times$ Å (with e the charge of an electron).[4] Of secondary importance is the intermolecular dipole-dipole repulsion, which dominates the interadsorbate interaction at high coverage where the average distance between adsorbates is short.[5] When two adsorbates are sufficiently close, they may tilt from their optimal geometry of the dispersed system in opposing directions between neighboring molecules in order to reduce the dipolar repulsion.[6] For sufficiently low coverage, where the dipolar interaction becomes negligible due to its $1/r^3$ dependence on the interadsorbate distance, the surface-mediated interactions start to dominate. A general feature of metal surfaces is the screening of an impurity charge on a characteristic length scale given by a Fermi wave vector k_f. The screening charge density, which takes the form of Friedel oscillations,[1,7] modulates the interadsorbate interaction between repulsion and attraction with a spatial period of π/k_f. This effect has been experimentally observed by measuring and analyzing the statistical distribution of interadsorbate separations,[8] where an optimal separation corresponding to the strongest attraction is found. Moreover, when the attraction is sufficiently strong, the interadsorbate distance becomes locked and the adsorbates are self-assembled into close-packed superlattices to gain most energy from the surface electron mediated interaction.[9]

For a substrate with undercoordinated atoms,[10–12] such as a reconstructed surface containing some empty sites, the situation becomes more complicated and the above picture may need some modification. The first consideration is the extra degrees of freedom: in the presence of undercoordinated atoms, there are multiple nonequivalent sites for the adsorption to take place, which opens the possibility of adsorption induced surface reconstruction. The surface reconstruction involves breaking original bonds and costs energy but, as mentioned previously, the adsorption is typically of the largest energy scale which determines the surface reconstruction. A typical example is CO adsorption on Pt(110) (1 × 2) reconstructed surface, where energy gain of CO binding at low coordination sites leads to step formation.[10,11] The second consideration is that the dispersion of surface electrons can be highly anisotropic, i.e., more one dimensional (1D), because with undercoordinated atoms it is more difficult for electrons to hop across the empty sites. The resulting surface mediated interadsorbate interactions can be greatly modified and become very directional.[13]

Feng *et al*.[14] have studied by low-temperature scanning tunneling microscopy (LT-STM) and density-functional theory (DFT) the CO adsorption on the anisotropic Cu(110)-(2 × 1)-O surface: the main purpose of the present work is to provide a coherent picture via a simple model to explain several unexpected observations, which include the strong adsorption induced surface distortion and nanograting self-assembly pattern of CO. The rest of this paper is organized as follows. In Sec. II we describe the system of interest and briefly review the main implications from Ref. 14. Important energy and length scales associated with CO adsorption subject to the experimental condition in Ref. 14 are also defined. In Sec. III we propose a simple microscopic model, derived mainly from density-functional theory (DFT), which captures the main

physics of the system. Within this model, we explain several key features of the observations. In Sec. IV the effective CO-CO interaction is calculated and the impact due to local CO adsorption is explicitly included. A simple microscopic picture is provided to account for the observed highly anisotropic inter-CO interaction. In Sec. V several features we neglect in the simple model are discussed. Finally conclusions are given. Some details of DFT and model calculations are given in the appendixes.

II. KEY FEATURES OF EXPERIMENTAL RESULTS

In Ref. 14 the LT-STM study of CO adsorption on the Cu(110)-(2 × 1)-O surface has been described. In this section we review the main experimental results of Ref. 14, the findings of DFT calculations, and discuss the important energy and length scales under the experimental conditions.

A. Main experimental observations

Figure 1(a) shows an STM image and the corresponding ball representation of the Cu(110)-(2 × 1)-O reconstructed surface, which is the substrate for CO chemisorption. The bright contrast corresponds to Cu atoms, which form added row Cu-O- chains above the bare Cu(110) surface. The Cu-O- chains extend along the ⟨001⟩ (defined as y) direction, and are separated from each other in the $\langle 1\bar{1}0\rangle$ (defined as x) direction by two substrate lattice constants corresponding to 5 Å [Fig. 1(a)].[15] In the ⟨001⟩ direction, Cu-O- chain has a lattice constant of 3.6 Å. The dosed CO is adsorbed only on Cu atoms of Cu-O- chains.[14] The most important feature of the Cu-O- chain is its one-dimensional electronic nature,[3,13,16] which is the key to several unexpected observations.

The experiment in Ref. 14 revealed an unusual CO molecule chemisorption behavior, which can be summarized as follows. For adsorption of an isolated CO molecule, both STM images and DFT calculations suggest that the CO pulls the host Cu atom by 1 Å from its equilibrium position. Moreover, the Cu-CO unit is tilted by 45° and it can interconvert between two degenerate tilted configurations on the STM imaging time scale (Fig. 2 in Ref. 14). For higher coverages, where CO molecules can interact, the effective inter-CO molecule potential is highly anisotropic: it is attractive along the x direction while being strongly repulsive along the y direction. These interactions lead to molecular self-assembly into a nanograting pattern [Fig. 1(b)]. As discussed in Ref. 14, the weakly attractive interaction can be explained by the interaction between tilted surface dipoles consisting of Cu-CO units. In the present work we will focus on two other striking features—the pronounced adsorption induced surface chain distortion, and the related medium range (>4 unit cells) intermolecular repulsion strictly localized on the same Cu-O- chain.

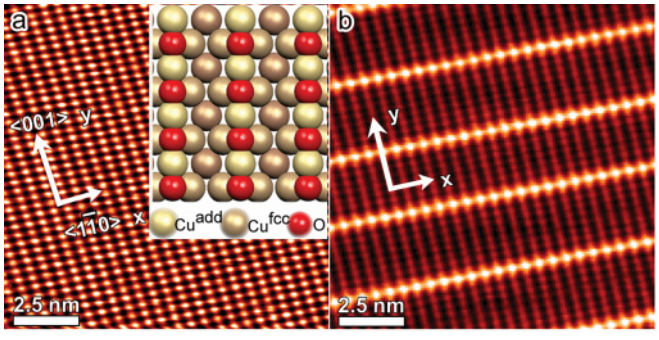

FIG. 1. (Color online) (a) STM image of Cu(110)-O surface. The bright contrast corresponds to the Cu atoms on Cu-O- chains. Inset shows the corresponding ball model of Cu(110)-O surface. The $\langle 1\bar{1}0\rangle$ and ⟨001⟩ are defined as x and y directions, respectively. The Cu-O- lattice constant is 3.6 Å whereas the interchain separation is 5 Å. (Inset) The ball model of Cu(110)-O surface. Cu^{fcc} represents Cu atoms of the Cu(110) substrate, and Cu^{add} represents Cu atoms of the top reconstructed Cu-O layer. (b) The self-assembled nanograting pattern after dosing CO onto the Cu(110)-O surface. The bright lines correspond to CO molecules: the CO-CO separation along x is 5 Å and the most probable interline distance is ∼26 Å.

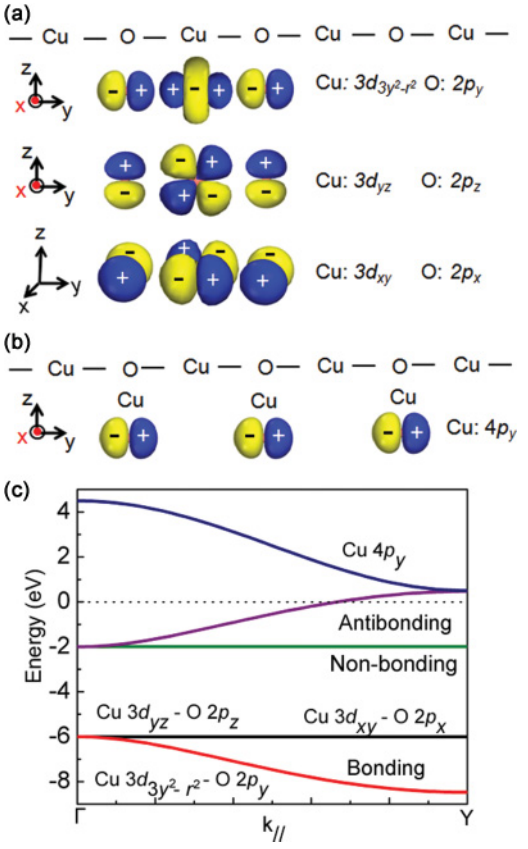

FIG. 2. (Color online) Orbitals close to the Fermi level, which are involved in CO-substrate interaction. (a) On the Cu-O- chain, Cu $3d_{3y^2-r^2}$ hybridizes with O $2p_y$ (σ type), Cu $3d_{yz}$ hybridizes with O $2p_z$ (π type), Cu $3d_{xy}$ hybridizes with O $2p_x$ (π type). (b) On the outmost layer of the Cu(110) surface, a surface band (Shockley surface state) composed of Cu $4p_y$ exists. (c) Seven tight-binding bands obtained from relevant orbitals described in (a) and (b). The σ-type hybridization leads to a bonding and an antibonding band whereas two π-type hybridizations are neglected leading to four flat nonbonding bands. Note that the highest two bands do not couple in the calculation shown here.

B. Important energy and length scales

Before proceeding to the model construction and calculations, definitions of the important energy and length scales of

the interadsorbate interaction established by the experimental temperature are needed. The energy scale associated with 77 K temperature of the experiments is 7 meV; it serves as a reference to compare with the energy and length scales of different interactions or dynamical processes. A length scale L_s is defined by intermolecular separation where the dipole-dipole interaction is comparable to the temperature. Taking the dipole moment of the Cu-CO unit (d) to be 0.26 $e\times$Å(see Sec. III D), L_s is thus estimated by $d^2/L_s^3 =$ 77 K $\sim$ 7 meV to be roughly 4.8 Å. This is the distance where the dipolar interaction is important and corresponds roughly to between one and two Cu-O- lattice constants along y.

Similarly, the energy scale for repulsive interaction-induced molecular desorption is defined by the temperature. According to Arrhenius equation, the desorption rate k of a single adsorbate is

$$k = fe^{-E_a/T}. \quad (1)$$

In this expression, the pre-exponential factor f is the attempt frequency for desorption, and $e^{-E_a/T}$ is the probability of each escaping attempt. The activation energy E_a can be decomposed into $E_a = -E_b - \Delta$ where $E_b(<0)$ is the single adsorbate binding energy (negative) whereas Δ is the interadsorbate interaction energy. Within our notation $\Delta > 0$ (<0) represents repulsive (attractive) interaction. The critical desorption rate, which marks the boundary of stable adsorption, can be defined as $k_0 = fe^{E_b/T}$ (therefore $k = k_0 e^{\Delta/T}$). If we define the criterion for strong interadsorbate interaction by $\Delta/T \gtrsim$ 2.3, which produces an order of magnitude increase in the desorption rate with respect to k_0, the critical energy scale for desorption at $T = 77$ K is $\Delta = 2.3 \times 77$ K $\sim$ 15 meV. This estimate implies that the CO-CO repulsion of $\sim$30 meV (because the interaction is shared by two adsorbates) is needed to destabilize the CO adsorption. Because of this repulsion-induced destabilization, the CO molecules in Fig. 1(b) are widely separated in the y direction.

III. MICROSCOPIC MODEL I: ADSORPTION INDUCED SUBSTRATE DISTORTION

In this section we construct a minimal model to explain the key features of experimental observations in Ref. 14. The model considers atomic orbitals close to the Fermi level (E_f), which are extracted from photoemission data,[13] tight-binding modeling,[16] and DFT calculations. After specifying the couplings between these relevant orbitals, which reasonably reproduce the observed bands on the Cu(110)-(2 $\times$ 1)-O surface, we provide a microscopic explanation for why CO induces a strong 1-Å lifting of the host Cu atom. A brief discussion on the CO-CO attraction along x, which is already described in Ref. 14, is also given for completeness.

A. Model of relevant substrate orbitals

In this and the next subsections we identify the most important electronic orbitals of the adsorbate-substrate system and construct a model by specifying couplings between them. The most relevant electronic orbitals are those close to E_f and can generally be inferred from the DFT calculation and the electron injection/removal experiments such as photoemission and STM. According to a tight-binding calculation,[16] the substrate orbitals involved in the bands close to E_f are Cu $3d_{3y^2-r^2}$, $3d_{yz}$, $3d_{xy}$, O $2p_y$, $2p_z$, $2p_x$ of the Cu-O- chain, and the Cu $4p_y$ of Cu(110) surface, as shown in Figs. 2(a) and 2(b). For orbitals on Cu-O- chains, symmetry allowed hoppings are between Cu $3d_{3y^2-r^2}$ and O $2p_y$ (σ bond), Cu $3d_{yz}$ and O $2p_z$ (π bond), as well as Cu $3d_{xy}$ and O $2p_x$ (π bond). Assuming there is no coupling between the Cu-O- chain and Cu(110) surface state (this restriction will be removed later) as in Ref. 16, a suitable choice of nearest-neighbor hoppings produces seven one-dimensional bands that disperse along the Γ-Y line of the surface Brillouin zone, as shown in Fig. 2(c), which reproduce the results of Ref. 16. Those calculated bands can be divided into three groups according to their interactions and symmetries: three Cu-O- bonding bands (one dispersive σ and two weakly dispersive π) between -6 and -8 eV; three Cu-O- antibonding bands between -2 eV and $+0.5$ eV; and one Cu $4p_y$ surface band above $+0.5$ eV. Photoemission measurements[13] confirm the lowest five bands and their 1D nature, whereas STM measurements[17] find another band with a minimum at $\sim$0.6 eV above E_f at the Y point. The σ antibonding band has never been described experimentally and a plausible explanation for its vanishing will be given shortly.

To construct a minimal model, we keep only the Cu-O- σ antibonding band and the Cu(110) $4p_y$ surface band, because they are closest in energy to the $2\pi^*$ bonding orbitals of CO molecules. As illustrated in Fig. 3(a), they are characterized by two tight-binding parameters t, t', an energy offset $E_{\rm off}$, and a coupling α. Note that the sign choice is to ensure the positive t, t', and α produce the correct dispersions. When $\alpha = 0$, the energy offset and the Fermi energy are chosen such that two bands touch at $+0.5$ eV at the Y point to comply with Ref. 16. When α becomes nonzero, these two bands couple most strongly at the Y point (due to the alternating sign), leading to level repulsion near the Y point. This coupling pushes the σ antibonding band down below E_f, where it

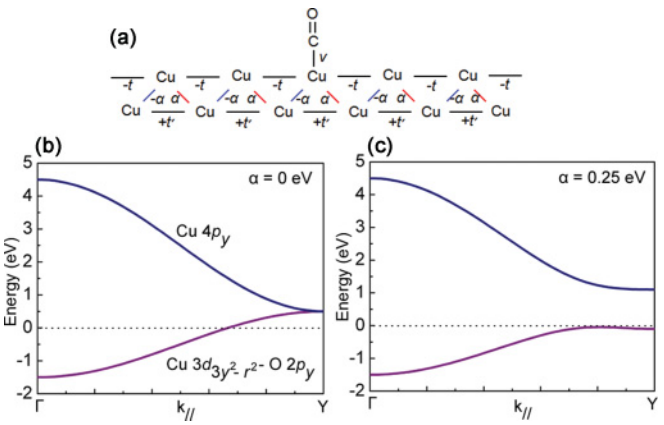

FIG. 3. (Color online) (a) The tight-binding coupling scheme used to model CO adsorption on Cu-O- chains. (b) The dispersions of the active surface bands without and (c) with their coupling ($\alpha =$ 0.25 eV). These two bands represent the top two bands in Fig. 2(c), which are retained in the minimal model for CO interaction with Cu(110)-O surface. In plots (b) and (c) $t = 0.5$ eV, $t' = 1$ eV are used and the bands are shifted such that $E_f = 0$ for $\alpha = 0$ eV.

has not been observed because it is now strongly coupled to the bulk bands of the substrate; whereas the Cu $4p_y$ surface state, now mixed with significant σ antibonding components, is pushed up and can be observed easily in STM measurements at 0.6 eV above E_f since it is inside the Y-projected band gap of the Cu(110) surface.[17] The effect of the coupling between the antibonding and $4p_y$ surface state bands is illustrated in Figs. 3(b) and 3(c).

The interactions just described can be represented by the Hamiltonian in the second quantization form

$$\begin{aligned} H_s = & -t\sum_{i,\sigma}(c^{\dagger}_{i,\sigma}c_{i+1\sigma} + \text{H.c.}) + t'\sum_{i,\sigma}(c'^{\dagger}_{i,\sigma}c'_{i+1,\sigma} + \text{H.c.}) \\ & + \sum_{i,\sigma}[\alpha(c^{\dagger}_{i,\sigma}c'_{i,\sigma} - c^{\dagger}_{i,\sigma}c'_{i-1,\sigma}) + \text{H.c.}] \\ & + \sum_{i,\sigma}[-\mu c^{\dagger}_{i,\sigma}c_{i,\sigma} + (E_{\text{off}} - \mu)c'^{\dagger}_{i,\sigma}c'_{i,\sigma}], \end{aligned} \tag{2}$$

where $c_{i,\sigma}$ and $c'_{i,\sigma}$ represent the σ antibonding orbital and the Cu(110) $4p_y$ orbitals. Chemical potential μ is introduced to describe the electron filling. Note that μ and E_f have exactly the same role but in our convention they differ by an offset: E_f is set to zero whereas μ is measured with respect to the middle point of the bare σ antibonding band described by the first term in Eq. (2). The subscript s in H_s represents "substrate." How to model the σ antibonding band by one effective hopping parameter is given in Appendix B. The offset energy is $E_{\text{off}} = 2t' + 2t$ so the two interacting bands touch at the Y point when $\alpha = 0$. As for the numerical values, we take $t = 0.5$ eV, $\mu = 0.4$ eV, $\alpha = 0.25$ eV to reproduce the results of Refs. 16, 13, and 17. The value of t' only slightly affects our subsequent energy calculations (see Sec. V) because the Cu $4p_y$ band is mostly empty, and we simply take $t' = t = 0.5$ eV.

B. Model of relevant CO orbitals and adsorption

We now proceed to discuss the relevant orbitals of CO and their couplings to the substrate. According to the Blyholder model,[18] chemisorption occurs through $2p_x$ and $2p_y$ orbitals of C; these orbitals combine into $2\pi^*$ molecular orbitals, which upon adsorption have the correct symmetry to hybridize with the host Cu $3d_{xz}$ and $3d_{yz}$ orbitals, as shown in Fig. 4(a). This picture is confirmed by DFT calculations. Figure 5 shows the projected density of states (PDOS) of CO $2\pi^*$ ($2p_y$ of C) and substrate Cu $3d_{yz}$ orbitals before and after the adsorption occurs. As shown in Fig. 5, without CO adsorption, which is simulated by putting CO 4 Å above the substrate Cu-O-chain, the CO $2\pi^*$ orbitals are $+1.5$ eV above E_f. When adsorption occurs, CO $2\pi^*$ is pushed up to $\sim$1.8 eV, and some of its weight appears below E_f due to its hybridization with the host Cu $3d$ orbitals. We will neglect the 5σ orbitals in our model whose effects will be discussed in Sec. V.

To model the adsorption in its simplest form, one needs two parameters—the energy of adsorbate ϵ_a (relative to the E_f) and its hybridization amplitude to the host orbital V. We will consider two cases: (i) there is only one adsorbate to describe single CO adsorption energy; and (ii) there are two adsorbates separated by R number of Cu-O- lattice constants to describe the substrate mediated interaction between two CO molecules. In the second quantization form, the Hamiltonians

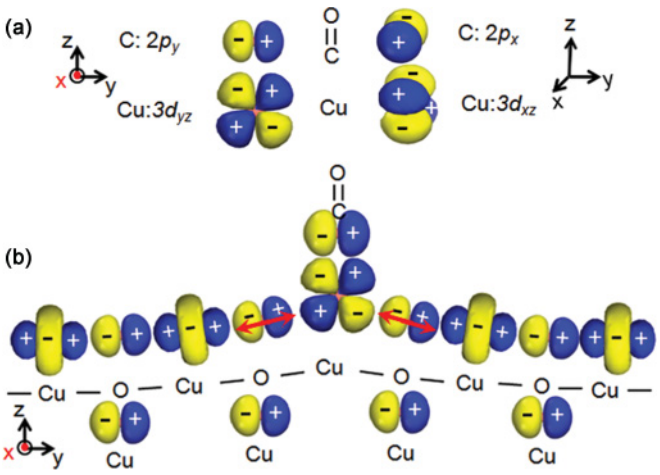

FIG. 4. (Color online) (a) CO adsorption channels: Hybridizations between CO $2\pi^*$ and Cu $3d$ orbitals are the main components contributing to CO adsorption. Left: C $2p_y$ and Cu $3d_{yz}$; right: C $2p_x$ and Cu $3d_{xz}$. (b) The relevant orbitals after CO adsorption: Without the lifting the relevant orbital of Cu atom is $3d_{3y^2-r^2}$, which forms strong bonds to adjacent O but cannot hybridize with CO $2\pi^*$ orbitals; by lifting the host Cu atom, the relevant orbital becomes $3d_{yz}$, which can simultaneously hybridize with CO $2\pi^*$ and O $2p_y$ orbitals. The arrows indicate the tilting directions of the O $2p_y$ orbitals that is required to maximize simultaneously the hybridization with the adjacent Cu $3d$ orbitals of the lifted Cu atom on one side and the Cu-O- chain on the other.

for one and two adsorbates are

$$\begin{aligned} H_a^{(1)}(R) &= \epsilon_a d_0^{\dagger}d_0, \\ H_a^{(2)}(R) &= \epsilon_a d_0^{\dagger}d_0 + \epsilon_a d_R^{\dagger}d_R, \end{aligned} \tag{3}$$

where the superscript (i) indicates the number of adsorbate, the subscript a stands for adsorbate, and d_j represents the molecular orbitals at site j. Hamiltonians describing the hybridization between adsorbate and substrate are

$$\begin{aligned} H_c^{(1)}(R) &= V(d_0^{\dagger}c_0 + \text{H.c.}), \\ H_c^{(2)}(R) &= V(d_0^{\dagger}c_0 + d_R^{\dagger}c_R) + \text{H.c.}, \end{aligned} \tag{4}$$

with the subscript c standing for coupling. According to the DFT PDOS result in Fig. 5, ϵ_a is 1.5 eV above E_f, and the CO-Cu coupling V is estimated to be 1 eV to give the calculated energy splitting. These parameters lead to an adsorption energy of 0.9 eV, which is roughly 50% larger than the 0.6 eV computed from DFT and inferred from a temperature programed desorption measurement.[19] One should bear in mind, however, that this estimate neglects the energy cost of the substrate distortion and the contributions from other possible interactions. The complete tight-binding description is summarized in Fig. 3(a). After specifying the model one can compute the adsorption energy and interadsorbate interaction using the formalism developed by Grimpley, Einstein, and Schrieffer (GES) in Refs. 20 and 21. The formalism, as it applies to CO chemisorption on Cu(110)-O surface, is presented in Appendix C.

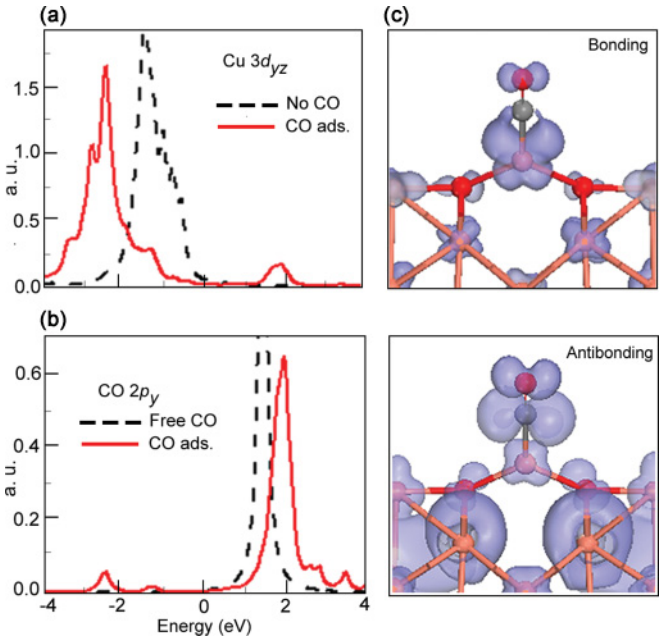

FIG. 5. (Color online) The PDOS in the arbitrary units (a.u.) for Cu $3d_{yz}$ (a) and CO $2p_y$ orbitals (b) with (solid) and without (dashed) CO adsorption plotted with respect to the Fermi level. In both calculations the host Cu is lifted 1 Å above its equilibrium position. For the case without CO adsorption, CO is placed at 4 Å above the lifted Cu. Adsorption of CO pushes CO $2p_y$ up to $+1.8$ eV with small weight transferred to -2 eV, whereas the Cu $3d_{yz}$ is pushed down to -2 eV with small weight transferred to $+1.8$ eV. The level repulsion and weight transfers are the consequence of hybridization between CO $2p_y$ and Cu $3d_{yz}$. (c) DFT calculations of constant charge-density surfaces for Cu $3d_{yz}$–CO $2p_y$ bonding (-2 eV, upper panel) and antibonding ($+1.8$ eV, lower panel) orbitals with CO adsorption and concomitant Cu lifting.

C. Adsorption induced substrate distortion

Based on the energy positions of relevant orbitals, we give a microscopic explanation why CO adsorption induces a 1-Å lifting of the host Cu. Generally the adsorption process gains energy from overlap of the orbitals of substrate atom and adsorbate; the closer the energy difference the larger the energy gain. This simple picture has been applied to several adsorbate/substrate systems to explain the adsorption induced surface reconstruction.[10,22] Here, the main hybridization channel is between CO $2\pi^*$ and Cu $3d_{yz}$ orbitals as illustrated in Fig. 4(a). The CO $2\pi^*$ and Cu $3d_{xz}$ interaction is relatively minor because of their large energy difference and will not be included in the discussion. From Fig. 2(c), the σ antibonding band, composed mainly of Cu $3d_{3y^2-r^2}$ orbitals, is closer to the CO $2\pi^*$ orbitals in energy than those composed of Cu $3d_{yz}$ and $3d_{xy}$, however, it has the wrong symmetry to form a bond with CO $2\pi^*$ orbitals. Pulling a Cu atom by around 1 Å from the chain enables the Cu $3d_{yz}$ orbital to hybridize simultaneously with *both* CO $2\pi^*$ and adjacent O p_y orbitals, as shown in Fig. 4(b). In this distorted Cu-O- chain configuration the $3d_{yz}$ orbital of the lifted Cu atom is incorporated in the σ antibonding band, effectively raising its energy closer to that of CO $2\pi^*$ orbitals, and consequently gaining more energy from hybridization.

It is also worth mentioning that although lifting the Cu atom stretches and thus slightly weakens the Cu-O bond (O $2p_y$ has larger overlap with the undistorted Cu $3d_{3y^2-r^2}$ orbital than lifted Cu $3d_{yz}$), this 1-Å lifting would be advantageous if the original surface were under a compressive strain due to its epitaxial relation with the substrate. This possibility is supported by the 1.849 Å Cu-O bond length in CuO_2, which is larger than 3.6/2 Å dimension of the substrate unit cell in the y direction.[23]

D. Tilted configuration and attractive dipolar interaction

STM measurements and DFT calculations show that in addition to the lifting, the chemisorbed CO molecule, including the host Cu atom, is tilted by $\sim\pm45^\circ$ with respect to surface normal (z direction) along the x direction.[14] One can attribute this Cu-CO tilting to the energy gain from the dipole-image dipole attraction and the negligible cost of rotating the Cu $3d$ orbitals at the adsorption site. We stress that it is the 1D character of the Cu-O- chain, which makes such tilting configuration possible. More specifically, as shown in Fig. 4(b), tilting the host Cu amounts to changing the local Cu $3d_{yz}$ orbital to $3d_{y'z'}$ with z' defined as 45° tilted with respect to the surface normal ($\hat{z'}\cdot\hat{z}=\hat{z'}\cdot\hat{x}=\cos 45^\circ$). In terms of the 1D Cu-O- chain, tilting a lifted Cu does *not* affect its hybridization amplitude with its adjacent O p_y orbitals and therefore preserves the electronic structure. The tilting would be energetically constrained if it involved breaking a chemical bond. Using our simple model with parameters previously specified, the adsorption involves a charge transfer from the Cu to CO, which is estimated to be $0.13e$. Because the charge transfer is mainly between Cu $3d$ and C $2p$ orbitals, whose mutual distance is roughly 2 Å, the surface dipole composed of Cu(+)-CO(−) unit can be estimated to be $0.26(=0.13\times 2)\ e\times$ Å, which is about twice as large at the value obtained by DFT calculation ($\sim 0.13\ e\times$Å).[14] Taking the image plane to be 0.5 Å *below* the Cu-O- chain,[24] the $\pm45^\circ$ CO configuration can gain an energy of $\sim$55 meV *more* from the dipole-image dipole interaction with respect to the 0° (vertical) CO configuration. The energy gain is roughly twice the value obtained from DFT calculation (difference between the vertical and tilted energy minima in Fig. 2(c) in Ref. 14). The DFT energy includes the repulsive interactions, such as the Pauli repulsion, which together with the attractive dipole-image dipole interaction, establish the 45° tilt angle.

The stable tilted CO adsorption also impacts the CO-CO interaction. Contrary to the repulsion between vertical surface dipoles, the CO-CO attraction between two 45° tilted dipoles leads to CO row formation in the direction of tilting, i.e., perpendicular to Cu-O- chains. At low CO coverage, STM measurements show the preference of CO molecules to form dimers and longer aggregates with two or more CO molecules located on adjacent Cu-O- chains tilting in the same direction, as expected from the *attractive* dipolar interaction.[14] The magnitude of energy gain due to tilting by a pair of dipoles can be estimated by computing the energy difference between two $+45^\circ$ tilted dipoles and two vertical dipoles with dipole moments of $0.26\ e\times$ Å and separation of 5 Å, which is roughly 10 meV. The dipolar energies for four different CO vertical and tilted pair configurations are given in Table I.

TABLE I. The dipolar energy for a pair of dipoles with different tilt angles. The reference (0 eV) is defined as the energy of two infinitely separated dipoles.

Dipole 1	Dipole 2	Energy (meV)
0°	0°	+7.35
0°	+45°	+3.5
+45°	+45°	− 3.6
+45°	−45°	− 2.9

IV. MICROSCOPIC MODEL II: SUBSTRATE DISTORTION INDUCED CO-CO REPULSION

In this section we explore the consequences of the proposed model for CO chemisorption to discuss the CO-CO interaction along the Cu-O- chain. In particular, we will show how the CO induced distortion leads to a strong CO-CO repulsion mediated by electronic interactions along the Cu-O- chain.

The strong lifting of the host Cu atom also causes moderate lifting of the chain atoms in its vicinity. Essentially these distortions occur to maximize the overlap between chain atoms close to the host Cu by *tilting* the nearby oxygen $2p_y$ and Cu $3d_{3y^2-r^2}$ orbitals *up* toward the lifted Cu atom, as illustrated in Fig. 4(b). When *two* CO molecules on the same Cu-O- chain are close, the chain cannot distort to optimize the electron hoppings *between* them as in the single CO molecule case, because the tilting direction favored by one of the CO is opposed to that favored by the other. For example, when two CO molecules are separated by one lattice constant, which is illustrated in Fig. 6(a), the direct Cu-O hoppings between Cu at site 0 and +1 become weaker than those outside the adsorbates, because the oxygen $2p_y$ orbital between site 0 and 1 does not tilt. Consequently the effective Cu-Cu

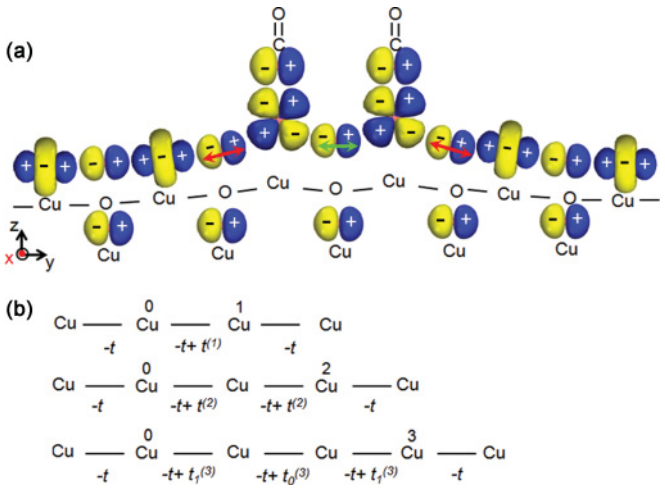

FIG. 6. (Color online) (a) The hopping suppression effect. When two CO molecules adsorb on the neighboring sites on the same Cu-O- chain, the overlap of Cu $3d_{yz}$ and O $2p_y$ orbitals along the Cu-O- chain is reduced by unfavorable geometry. Two tilted (red) arrows indicate the tilting directions of the O $2p_y$ orbitals to maximize hybridization with $3d$ orbitals of adjacent Cu atoms. The horizontal (green) arrow indicates that the O $2p_y$ sandwiched by two lifted Cu cannot tilt. (b) The tight-binding model of the relevant orbital interactions.

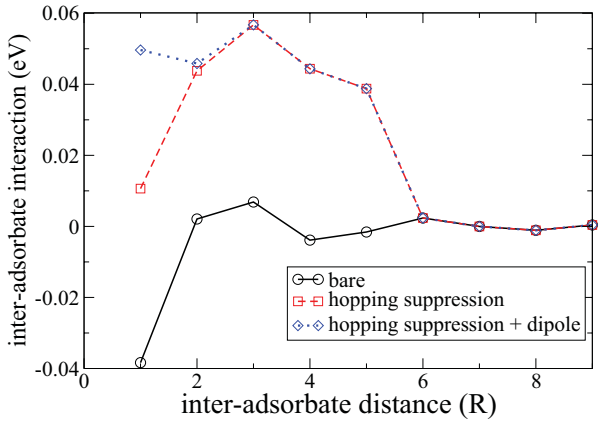

FIG. 7. (Color online) The interadsorbate interaction as a function of inter-CO distance. The dashed and solid curves are chain-mediated interactions with and without the hopping suppression, respectively; the dotted curve includes both the hopping suppression and the dipole-dipole repulsion. Without the hopping suppression and dipolar repulsion, the GES model predicts a bound state between pairs of adsorbates at $R = 1$ (Ref. 21).

hopping along the chain segment between two neighboring CO molecules is suppressed; we name this mechanism the *hopping-suppression* effect.

Figure 6(b) illustrates how the effective Cu-Cu hopping is modified due to the hopping suppression. Details of the model parameters are provided in Appendix D and here we simply discuss the results. In the case of 77-K experiments, as discussed in Sec. III B, a repulsion energy of ∼30 meV is necessary to prevent proximate adsorption of two CO molecules on the same Cu-O- chain. Figure 7 shows the effective CO-CO interaction mediated by substrate electrons. The hopping suppression-induced repulsion affects CO adsorption for the inter-CO distance $R = 1$–5 in Cu-O unit cells. For $R = 2$–5, the repulsion energy is greater than 38 meV, i.e., five times larger than the experimental temperature at 77 K. At $R = 1$, however, the GES model *without* hopping suppression predicts a strong bound state,[21] and therefore including the hopping suppression results in an effective repulsion of only 11 meV. At this distance, however, the short-range dipole-dipole repulsion is significant and has to be included. Estimating the same dipole moment as used to explain CO row formation, the repulsion energy at $R = 1$ for two parallel CO molecules at a distance of 3.6 Å is ∼20 meV. Combining both mechanisms for intermolecular repulsion our model predicts stable chemisorption for a minimum separation of 5 lattice constants (∼18 Å) between two CO molecules.

According to our model, the main effect of the hopping suppression is that two proximate adsorbates on the same Cu-O- chain effectively divide the 1D substrate into two segments. To put it simply, one adsorbate loses interaction with half of the substrate by presence of another, which reduces the a *single molecule* adsorption energy. Such segmenting, which is only possible for a 1D substrate, has been recently reported in the interaction of single CO molecule with a single-atom wide Au chain.[25] The range of repulsion depends on the extent of the adsorption-induced substrate distortion. Our calculation only considers this effect for intermolecular separation $R \leqslant 5$ and

within this range a strong repulsion is found. We point out that the hopping suppression repulsion requires only Cu atom lifting and is not related to the Cu-CO unit tilting.

V. DISCUSSION

Having proposed the hopping suppression model, which successfully accounts for the on-chain repulsion between CO molecules, here we first discuss the sensitivity of the model to various parameters, and then justify the neglected interactions in our model. Included in our model are the substrate electronic bands [Eq. (2)], the interaction of one or two adsorbates with the substrate [Eqs. (3) and (4)], and the substrate mediated interaction between adsorbates that leads to the hopping suppression [Fig. 6 and Eq. (D1)].

The substrate is described by two bands and five parameters [Eq. (2)]. As discussed in Sec. III A, based on a previous tight-binding calculation[16] we use $t = t' = 0.5$ eV, $\alpha = 0.25$ eV, $\mu = 0.4$ eV, and $E_{\rm off} = 2$ eV. For the adsorption energy calculation, only two of these five parameters are important–the hopping parameter of the partially filled band t, and the chemical potential μ, because the upper substrate band is empty. If we take the coupling $\alpha = 0$, which reduces the problem to a one-band model (t' and $E_{\rm off}$ become irrelevant), the difference from the presented results is smaller than 15% (the one band model leads to larger adsorption energy). We note, however, that all five parameters are needed to explain the observed peak $\sim$0.6 eV above E_f in STM measurements.[19]

The adsorbate-substrate interaction is described by two parameters: the energy of the $2\pi^*$ state from the DFT PDOS (Fig. 5), for which we choose $\epsilon_a = 1.5$ eV [Eq. (3)], and the interaction strength $V = 1$ eV [Eq. (4)]. From a second-order perturbation calculation estimate, the adsorption energy is approximately V^2/ϵ_a. Finally, the hopping suppression [Eq. (D1)] is described by only one parameter (see the discussion in Appendix D). Numerically we found that for interadsorbate separation $R > 1$ lattice constant, a hopping reduction of $\lesssim$10% is enough to produce the required repulsion (in the sense of Sec. II B). For $R = 1$, without hopping suppression two adsorbates experience a strong attraction due to the bound-state formation (Sec. IV and Fig. 7). In this case a hopping suppression of $\gtrsim$30% and the dipolar repulsion are needed. Overall when $R \geqslant 2$, the required repulsion can be achieved easily, without invoking the additional dipole-dipole repulsion.

Our model also does not include the hybridization of the CO 5σ orbitals with the substrate, which is often invoked in the Blyholder-type interaction. The orbital is deep (roughly -6 eV below E_f), and therefore the main effect of its interaction is the Pauli repulsion with the occupied bands of the substrate.[26–28] As we noted in Ref. 14, Pauli repulsion may contribute to lifting of the host Cu atom, and slightly reduces the single adsorption energy, but does *not* contribute to the interadsorbate interaction[21] because the surface band is completely filled. Because we focus here on surface-mediated interaction, the 5σ orbital is not included in our model.

Including the Van der Waals interaction in DFT[29] has been shown to supplement chemisorption in the characterization of some adsorbate systems.[29–31] In the present DFT calculation the Van der Waals effect is not included, but reasonable agreement with experiments[14] is reached. Therefore we believe this effect does not significantly affect the CO molecule self-assembly as a first approximation. Our preliminary calculations show that the Van der Waals interaction indeed increases the chemisorption energy by 0.1–0.2 eV depending on the CO molecule geometry,[32] but it does not alter the chemisorption structure that is responsible for the self-assembly.

Finally, we consider the elastic energy associated with the chemisorption. The elastic energy typically describes the energy cost of a *small* lattice distortion where the local orbitals contributing to the bonding essentially remain intact. In the case where CO induces a *large* distortion, however, such as the 1-Å lifting of the host Cu atom (Sec. III C), the existing bonds (Cu $3d_{3y^2-r^2}$ and O $2p_y$) are broken and new bonds are formed (Cu $3d_{yz}$ and O $2p_y$). In this case, the elastic energy with respect to the undistorted chain imposes an energy barrier between the initial undistorted and the final strongly distorted configurations, but is *not* directly related to the energy of the final configuration. In fact, in the DFT calculation starting from the undistorted configuration and allowing the system to relax, the 1-Å Cu lifting configuration is attained without an energy barrier. This suggests that the elastic energy cost of forming the chemisorption bond is only a secondary energy scale, and including only the electronic contribution is sufficient for the current purpose.

VI. CONCLUSION

We have proposed and implemented a simple model to explain the striking features of CO adsorption on a Cu(110)-(2 × 1)-O surface that emanate from the undercoordinated nature of the adsorption sites and one-dimensional electronic properties of the substrate. A coherent picture of CO chemisorption on the Cu(110)-(2 × 1)-O surface can be summarized as follows. First, CO adsorption induces a strong host Cu lifting of 1 Å because this distortion effectively moves the Cu $3d_{yz}$ orbital up in energy and consequently gains more energy from Cu $3d_{yz}$ and CO $2\pi^*$ hybridization. This is the primary manifestation of the interaction of CO molecules with the 1D substrate. Moreover, the CO adsorption prefers a 45° tilted configuration because it allows for the dipole-image dipole attraction. The 1D nature of the substrate ensures that no bonds are broken for all tilt angles (like a hinge), which could not happen for an isotropic 2D substrate. The unusual chemisorption geometry of CO molecules on Cu-O- chains involving both lifting and tilting leads to very anisotropic CO-CO interactions. Along the x direction, CO molecules have a tendency to form rows because of attraction between 45° tilted dipoles, whereas in the perpendicular y direction, CO molecules tend to repel one another because of the hopping suppression effect. The nanograting self-assembly pattern is a graphic manifestation of these two anisotropic interactions. Note that although the inter-CO interaction is governed by different mechanisms, which lead to orthogonal attractive and repulsive interactions, they are both direct consequences of the strong lifting of host Cu atom upon CO chemisorption.

Our work illustrates how formation of a chemical bond through specific orbital interactions between an adsorbate and 1D dispersive states of the substrate can impact the surface geometrical and electronic structures. In particular for the 1D

or quasi-1D substrate surfaces, the *vertical* displacement of the adsorbate can be crucial. We expect that similar chemisorption-induced restructuring could be favorable at step and kink defects on 2D surfaces and other reduced coordination sites that may confer enhanced catalytic properties.

ACKNOWLEDGMENTS

We thank G. Benedek for discussions, DOE-BES Division of Chemical Sciences, Geosciences, and Biosciences for support through Grant No. DE-FG02-09ER16056, W. M. Keck foundation, Ministerio de Cienciae Innovación (Grant No. FIS2010-19609-C02-00) and G.V.-UPV/EHU (Grant No. IT-366-07) for financial support. Some calculations were performed in the Environmental Molecular Sciences Laboratory at the PNNL, a user facility sponsored by the DOE Office of Biological and Environmental Research.

APPENDIX A: DETAILS OF DFT CALCULATION

DFT calculations were performed using the VASP code[33] with a well converged 500.0-eV plane-wave cutoff, the Perdew-Wang functional,[34] and the projector augmented wave method.[35] The Cu substrate was represented by a slab containing ten layers and, for all the lateral supercells considered, the number of k points was always consistent with a $3 \times 4 \times 1$ k sampling of the underlying (2×1) substrate unit cell.

APPENDIX B: MODELING THE SUBSTRATE BANDS

First, we discuss how to model the antibonding Cu-O-band by the tight-binding model with only one effective Cu-Cu hopping on the Cu-O- chain. As shown in Fig. 2(a), without CO adsorption the *direct* hoppings from an oxygen $2p_y$ to its left and right Cu $3d_{3y^2-r^2}$ have the opposite signs. Assuming the energy difference between Cu and O orbitals is $\Delta E(>0)$ and the hopping amplitude t_{pd}, the dispersion of the antibonding band is $\frac{\Delta E}{2} + \{(\frac{\Delta E}{2})^2 + 2t_{pd}^2[1-\cos(k)]\}^{1/2}$.[13] When $|t_{pd}/\Delta E| \ll 1$, the antibonding band dispersion can be approximated with $-2(\frac{t_{pd}^2}{\Delta E})\cos(k)$ (discarding an overall energy shift), from which we deduce that the effective Cu-Cu hopping is $-t$ where $t = \frac{t_{pd}^2}{\Delta E}$. Generally the effective hopping between two adjacent Cu is given by $-t$ with

$$t = -t_{pd,L} \times t_{pd,R}/\Delta E, \tag{B1}$$

where $t_{pd,L(R)}$ is the direct hopping between the O $2p$ orbital and its left (right) Cu $3d$ orbital. The Cu(110) surface band is characterized by $+t'$, which is the *direct* Cu $4p_y$–Cu $4p_y$ hopping. The sign choice in Fig. 3 makes both t and t' positive. Similar to the effective Cu-Cu hopping for the Cu-O-antibonding band, the coupling between Cu atoms on Cu-O-chain and Cu on the Cu(110) surface is also mediated via hoppings through oxygens. Because the equation is similar to Eq. (B1), the couplings alternate in sign as shown in Fig. 3(a).

APPENDIX C: HAMILTONIAN AND FORMALISM

The Hamiltonian we use to describe the effective adsorbate-substrate interaction is divided into three parts—the substrate, the absorbates, and the coupling between them:

$$H^{(i)} = H_0^{(i)} + H_c^{(i)} \equiv \left(H_s + H_a^{(i)}\right) + H_c^{(i)}. \tag{C1}$$

As discussed in Secs. III A and III B, the superscripts $i = 1$ or 2 indicate the number of absorbates considered, and the subscripts s, a, and c stand for substrate, adsorbate, and coupling, respectively. The exact forms are specified in Eqs. (2)–(4) and Eq. (D1). Equation (C1) is quadratic in fermionic operators and therefore can be solved exactly. To compute the adsorption energy, we denote the eigenvalues of $H_0^{(i)}$ and $H^{(i)}$ as $\epsilon_{0,j}$ and ϵ_j and the energy gain from the absorption is

$$\Delta W = \sum_{\epsilon_{j<E_f}} \epsilon_j - \sum_{\epsilon_{j<E_{0,f}}} \epsilon_{0,j}, \tag{C2}$$

with $E_f(E_{0,f})$ the Fermi level of interacting (noninteracting) system. Note that because the number of adsorbates is negligible (one or two over many electrons) compared to that of conduction electrons, $E_{0,f} = E_f$.[21,36] E_f is therefore determined by the density of *bare* surface conduction electron n, i.e.,

$$n = \frac{1}{N}\sum_j \Theta(E_f - \epsilon_{0,j}), \tag{C3}$$

where N is the total number of sites and $\Theta(x)$ is the step function [$\Theta(x) = 1$ (0) when x is positive (negative)]. The value of E_f remains fixed when coupling to the adsorbates.

Following the derivation in Ref. 21, we define the bare Green's function $G_0^{(i)}(E) = [E - H_0^{(i)}]^{-1}$ and the absorption energy is given by

$$\Delta W = -\frac{2}{\pi}\int_{-\infty}^{E_f} dE\ \mathrm{Imln}\left[I - G_0^{(i)}(E)V^{(i)}\right]. \tag{C4}$$

The single molecule adsorption energy is

$$\Delta W_{\mathrm{single}} = -\frac{2}{\pi}\int_{-\infty}^{E_f} dE\ \mathrm{Imln}\left[I - G_0^{(1)}(E)V^{(1)}\right]. \tag{C5}$$

The interaction between a pair of adsorbates as a function of separation R is

$$\Delta W_{\mathrm{pair}}(R) = -\frac{2}{\pi}\int_{-\infty}^{E_f} dE\ \mathrm{Imln}\left[I - G_0^{(2)}(E)V^{(2)}(R)\right] - 2W_{\mathrm{single}}. \tag{C6}$$

Note that the repulsive (attractive) interaction depending on the interadsorbate distance corresponds to $\Delta W_{\mathrm{pair}}(R) > 0$ [$\Delta W_{\mathrm{pair}}(R) < 0$].

APPENDIX D: MODEL OF HOPPING SUPPRESSION

As illustrated in Fig. 3(b), the amplitude of electron hoppings on the same Cu-O chain between two CO molecules is reduced from t to $t - t^{(i)}$, and the amount of hopping suppression is determined as follows. First, we recall from Eq. (B1) that t, the effective Cu-Cu hopping without distortions and the reference value for comparing suppression, is given by $t_{pd} \times t_{pd}/\Delta E$ with t_{pd} the direct Cu-O hopping without CO adsorption. Here we use the notation where $-t_{i-j}$ represents the effective electron hopping between site i and j. Because

the sign of hopping effect has no real influence for the current purpose, we assume that t_{i-j} is always positive and take the absolute value of Eq. (B1) when evaluating the hoppings.

For two adsorbates separated by one lattice constant ($R = 1$), we *assume* the direct oxygen-copper hopping $t_{p_y d_{xz}} = 0.8t_{pd}$ for the oxygen *between* Cu at site 0 and 1, leading to an effective hopping $t_{0-1} = 0.64t = t - t^{(1)}$ and therefore $t^{(1)} = +0.36t$. The justification will be given shortly. We emphasize that to comply with the assumption that a single Cu lifting does not change the substrate band dispersion, the effective hoppings outside two CO molecules are the same as those without CO adsorption. For $R > 1$, we further approximate the suppressed *direct* hopping by

$$\tilde{t}_{pd}(L) = t_{pd}\left[1 - \gamma\frac{1\text{Å}}{L}\right], \tag{D1}$$

with 1 Å the vertical displacement of the host Cu, L half the horizontal separation between two host Cu, and γ, a constant, set to 0.36 so that when $L = 1.8$ Å, $\tilde{t}_{pd} = 0.8t_{pd}$, which reduces to the $R = 1$ case. This expression approximates the tilting angle of the linear orbital (Cu $3d_{3y^2-r^2}$ or O $2p_y$) to be $\tan^{-1}[1\,\text{Å}/L]$ and at large L ($L > 3.6$ Å) it amounts to that the direct $d - p$ hopping reduces linearly as a function of the tilting angle.[37]

For $R = 2$, the Cu-O hoppings from Cu at site 0 to its right oxygen, and from site 2 left are unchanged due to the tilting of oxygen p_y orbital, but the Cu-O hoppings from Cu at site 1 to its adjacent oxygens are suppressed because the tilting of Cu $3d_{3y^2-r^2}$ can only maximize the hopping to one direction. Applying Eq. (D1), this hopping is $\tilde{t}_{pd}(L = 3.6\,\text{Å}) = 0.9t_{pd}$ leading to $t_{0-1} = t_{1-2} = 0.9t$ and $t^{(2)} = +0.1t$. For $R = 3$, we have $t_{0-1} = t_{2-3} = t$ and thus $t_1^{(3)} = 0$. The Cu-O hopping between O and Cu at site 1 and 2 is to be $\tilde{t}_{pd}(L = 5.4\,\text{Å}) = 0.93t_{pd}$, leading to $t_{1-2} = 0.87t$ and $t_0^{(3)} = 0.13t$. The same arguments could be used to estimate the hopping suppression for $R > 3$, as appears to be important in the experiment, and here we model this effect up to $R = 5$.

Similar hopping suppression has been implicated in the transport properties of manganites, which undergo Jahn-Teller distortion. As seen in the $LaMnO_3$,[37] the $GdFeO_3$-type rotation pushes the O between two adjacent Mn away from the Mn-Mn axis, thereby reducing the hybridization of Mn $3d$ e_g and O $2p$ orbitals. Such distortion can reduce the effective Mn-Mn hopping by 40% (corresponding to the direct Mn-O hopping reduction by 20%) when the Mn-O-Mn angle is 150° (for the unperturbed structure, the angle is 180°). Because in the current case, the lobes of the lifted Cu $3d_{yz}$ and its adjacent O $2p_y$ orbitals are not pointing toward each other, we therefore believe that although the values of hopping suppression used here are assumed, our estimates are conservative.

*Present address: Department of Physics, University of Texas at Austin, Texas 78712.

[1] M. Ternes, M. Pivetta, F. Patthey, and W.-D. Schneider, Prog. Surf. Sci. **85**, 1 (2010).

[2] P. R. Antoniewicz, Phys. Rev. Lett. **32**, 1424 (1974).

[3] H. Kuhlenbeck and H. J. Freund, *Electronic Structure*, edited by K. Horn and M. Scheffler, Vol. 2 (Elsevier, Amsterdam, 2000), pp. 670–747.

[4] T. C. Leung, C. L. Kao, W. S. Su, Y. J. Feng, and C. T. Chan, Phys. Rev. B **68**, 195408 (2003).

[5] I. Fernandez-Torrente, S. Monturet, K. J. Franke, J. Fraxedas, N. Lorente, and J. I. Pascual, Phys. Rev. Lett. **99**, 176103 (2007).

[6] H. Kato, H. Okuyama, S. Ichihara, K. Maki, and J. Yoshinobu, J. Chem. Phys. **112**, 1925 (2000).

[7] J. Friedel, Nuovo Cimento Suppl. **7**, 287 (1958).

[8] J. Repp, F. Moresco, G. Meyer, K.-H. Rieder, P. Hyldgaard, and M. Persson, Phys. Rev. Lett. **85**, 2981 (2000).

[9] F. Silly, M. Pivetta, M. Ternes, F. Patthey, J. P. Pelz, and W.-D. Schneider, Phys. Rev. Lett. **92**, 016101 (2004).

[10] P. Thostrup, E. Christoffersen, H. T. Lorensen, K. W. Jacobsen, F. Besenbacher, and J. K. Nørskov, Phys. Rev. Lett. **87**, 126102 (2001).

[11] P. Thostrup, E. K. Vestergaard, E. Lægsgaard, and F. Besenbacher, J. Chem. Phys. **118**, 3724 (2003).

[12] D. Loffreda, L. Piccolo, and P. Sautet, Phys. Rev. B **71**, 113414 (2005).

[13] R. Courths, B. Cord, H. Wern, H. Saalfeld, and S. Hüfner, Solid. State. Commun. **63**, 619 (1987).

[14] M. Feng, P. Cabrera-Sanfelix, C. Lin, A. Arnau, D. Sánchez-Portal, J. Zhao, P. Echenique, and H. Petek, ACS Nano **5**, 8877 (2011).

[15] M. Feng, J. Lee, J. Zhao, J. T. Yates Jr., and H. Petek, J. Am. Chem. Soc. **129**, 12394 (2007).

[16] L. H. Tjeng, M. B. J. Meinders, and G. A. Sawatzky, Surf. Sci. **233**, 163 (1990).

[17] C. Corriol, J. Hager, R. Matzdorf, and A. Arnau, Surf. Sci. **600**, 4310 (2006).

[18] H. Blyhoder, J. Phys. Chem. **68**, 2772 (1964).

[19] J. Ahner, D. Mocuta, and J. T. Yates Jr., Surf. Sci. **390**, 126 (1997).

[20] T. B. Grimley, Proc. Phys. Soc. **90**, 751 (1967).

[21] T. L. Einstein and J. R. Schrieffer, Phys. Rev. B **7**, 3629 (1973).

[22] B. Hammer, Y. Morikawa, and J. K. Nørskov, Phys. Rev. Lett. **76**, 2141 (1996).

[23] E. Ruiz, S. Alvarez, P. Alemany, and R. A. Evarestov, Phys. Rev. B **56**, 7189 (1997).

[24] J. Zhao, N. Pontius, A. Winkelmann, V. Sametoglu, A. Kubo, A. G. Borisov, D. Sánchez-Portal, V. M. Silkin, E. V. Chulkov, P. M. Echenique *et al.*, Phys. Rev. B **78**, 085419 (2008).

[25] N. Nilius, T. M. Wallis, and W. Ho, Phys. Rev. Lett. **90**, 186102 (2003).

[26] R. Hoffmann, Rev. Mod. Phys. **60**, 601 (1988).

[27] A. Föhlish, M. Nebergy, P. Bennich, L. Triguero, J. Hasselström, O. Karis, L. G. M. Pettersson, and A. Nilsson, J. Chem. Phys. **112**, 1946 (2000).

[28] P. S. Bagus, C. J. Nelin, and C. W. Bauschlicher, Phys. Rev. B **28**, 5423 (1983).

[29]M. Dion, H. Rydberg, E. Schröder, D. C. Langreth, and B. I. Lundqvist, Phys. Rev. Lett. **92**, 246401 (2004).
[30]K. Berland, T. L. Einstein, and P. Hyldgaard, Phys. Rev. B **80**, 155431 (2009).
[31]S. D. Chakarova-Käck, O. Borck, E. Schröder, and B. I. Lundqvist, Phys. Rev. B **74**, 155402 (2006).
[32]H. Sun and J. Zhao (unpublished).
[33]G. Kresse and J. Furthmüller, Phys. Rev. B **54**, 11169 (1996).
[34]J. P. Perdew, J. A. Chevary, S. H. Vosko, K. A. Jackson, M. R. Pederson, D. J. Singh, and C. Fiolhais, Phys. Rev. B **46**, 6671 (1992).
[35]P. E. Blöchl, Phys. Rev. B **50**, 17953 (1994).
[36]P. W. Anderson, Phys. Rev. **124**, 41 (1961).
[37]C. Ederer, C. Lin, and A. J. Millis, Phys. Rev. B **76**, 155105 (2007).